AD-A126 586 HIGH PASS FILTERING OF SATELLITE ALTIMETER DATA(U) 1/1

NAVAL SURFACE WEAPONS CENTER DAHLGREN VA B ZONDEK

OCT 82 NSWC/TR-82-427

UNCLASSIFIED F/G 8/7 NL

END

DATE FILMED

4 - 83

DTIC

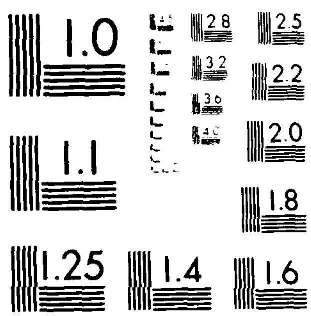

MICROCOPY RESOLUTION TEST CHART

UNCLASSIFIED

SECURITY CLASSIFICATION OF THIS PAGE (When Data Entered)

REPORT DOCUMENTATION PAGE		READ INSTRUCTIONS BEFORE COMPLETING FORM
1. REPORT NUMBER NSWC TR 82-427	2. GOVT ACCESSION NO. A126 586	3. RECIPIENT'S CATALOG NUMBER
4. TITLE (and Subtitle) HIGH PASS FILTERING OF SATELLITE ALTIMETER DATA		5. TYPE OF REPORT & PERIOD COVERED
		6. PERFORMING ORG. REPORT NUMBER
7. AUTHOR(s) B. Zondek		8. CONTRACT OR GRANT NUMBER(s)
9. PERFORMING ORGANIZATION NAME AND ADDRESS Naval Surface Weapons Center (K104) Dahlgren, Va. 22448		10. PROGRAM ELEMENT, PROJECT, TASK AREA & WORK UNIT NUMBERS
11. CONTROLLING OFFICE NAME AND ADDRESS Defense Mapping Agency Washington, DC 20305		12. REPORT DATE October 1982
		13. NUMBER OF PAGES 23
14. MONITORING AGENCY NAME & ADDRESS(if different from Controlling Office)		15. SECURITY CLASS. (of this report) UNCLASSIFIED
		15a. DECLASSIFICATION DOWNGRADING SCHEDULE

16. DISTRIBUTION STATEMENT (of this Report)

Approved for public release; distribution unlimited.

17. DISTRIBUTION STATEMENT (of the abstract entered in Block 20, if different from Report)

18. SUPPLEMENTARY NOTES

19. KEY WORDS (Continue on reverse side if necessary and identify by block number)

Altimeter
Satellite
Tectronics

20. ABSTRACT (Continue on reverse side if necessary and identify by block number)

A numerical-graphical method is described to extract weak mesoscale signatures from Seasat altimeter data. Results are presented in a form suitable for overlay on a Mercator grid. The signatures presented are thought to be due to tectonic anomalies.

DD FORM 1 JAN 73 1473 EDITION OF 1 NOV 65 IS OBSOLETE
S/N 0102-LF-014-6601

UNCLASSIFIED

SECURITY CLASSIFICATION OF THIS PAGE (When Data Entered)

FOREWORD

This work was sponsored by the Defense Mapping Agency.

The author wishes to express his appreciation to R. J. Anderle, D. R. Brown, Jr., C. A. Fisher, C. W. Duke, Jr., and R. L. Kulp of the Space and Surface Systems Division for their generous support and encouragement.

Computer programming was most ably carried out by H. Castro (now deceased) and J. B. Ellis.

Released by:

O. F. BRAXTON, Head
Strategic Systems Department

ACKNOWLEDGMENT

We thank the staff of NSWC for much assistance. The computer graphics package was prepared by John Walker of Sperry-Univac.

CONTENTS

ABSTRACT

A numerical-graphical method is described to extract weak mesoscale signatures from Seasat altimeter data. Results are presented in a form suitable for overlay on a Mercator grid. The signatures presented are thought to be due to tectonic anomalies.

INTRODUCTION

Low pass filtering of satellite altimeter data to estimate sea surface topography and slope has been discussed by various authors [1,2,3]. These methods tend to smooth out some physically meaningful signatures embedded in the data, especially those of small scale. In order to bring out these signatures that are not far above the noise level, it is useful to pass the data through a high pass filter. The digital filters we have considered have half amplitudes in the range of some hundreds of kilometers. This implies that the contribution due to the imprecision in the satellite's position determination (the ephemeris error) is filtered out. Application of the formulas derived in [4], yields the result that ephemeris noise power at these short wavelengths is far below the altimeter noise level (~10 cm).

We summarize below some of the uses to which high pass altimeter data filtering may be put:

a. Tectonic detection:

Seamount detection

Detection of signatures of elongated features extending across many parallel altimeter data tracks. These signatures may be so weak in relation to the noise as to become apparent only by correlation across tracks. Examples will be given.

b. High pass filtering is a useful tool in data editing. Isolated data errors (perhaps due to a dropped bit in the data transmission) and of small magnitude in relation to the unfiltered data (geoid height, in our case) are made to stand out conspicuously. An automatic data editing procedure might be based on a judiciously chosen filter. Examples of data error detection will be given.

RECURSIVE DIGITAL FILTERS

The data volume to be processed in a systematic coverage of the oceans is formidable, and therefore computational efficiency is an important consideration. Since we are not searching for a well-defined signature, there is no well-defined optimal filter. We have considered the digital Butterworth filters [5]. They have the advantage of great simplicity, and their frequency response functions have no ripples. Applying the filter recursion in a forward and backward sweep removes the phase [6, p. 194].

A disadvantage of recursive filters lies in the appearance of end effects, i.e., transients near the ends of the data span. The higher the filter order and the wider the frequency pass band, the greater the end effects. In Figure 1 we have plotted the frequency response functions of the back and forth sweep Butterworth filters for some typical cases.

The Seasat altimeter data are available to us as sampled values spaced at about 3.32 km (the results of averaging over 500 separate altimeter readings).

The family of high pass filters which we are considering involves two adjustable parameters. the order, N, and half power wavelength, λ (equal to the half amplitude wavelength for the back and forth sweep).

The proper choice of these parameters depends on a number of factors:

a. The scale of the tectonic features we are looking for, projected along the subtrack. For elongated features this involves the angle between the axis of the feature and the subtrack.

b. Control of data gap transients: Due to the finite data spans (dry land and other causes), transients are excited which one would like to limit to a small neighborhood of the data gaps. For fixed λ, larger transients are associated with high order, N.

c. Resolution of neighboring signatures: The larger the order N, the steeper the attenuation of the frequency response but the slower the decay of the impulse response. This leads to poor resolving capability for high order filters.

The filtered data have been plotted along normals to the subtracks on a Mercator grid. This makes these charts suitable for overlay on other charts (bathymetry, basement charts, magnetic anomalies). The North-East to South-West (descending) tracks have positive values to the left, the South-East to North-West (ascending) to the right. The normal scale has been chosen so that 1 meter of geoid height corresponds to 1° of longitude in the grid.

In the following section we discuss some sample results. We make no attempt at quantitative correlation of signatures and tectonics.

SOME TECTONIC SIGNATURES

In Figure 2 is reproduced a bathymetric chart in the Mid-Pacific Seamount province [7, chart 1803 N].

In Figure 3 one observes along track 1164 and its repeats (thick line), a "Seamount Signature" at 12° 55′ N, 174° 8′ W that does not correlate with the bathymetry. Along tracks 131 and 619 one notices "Seamount Signatures" at 13° 55′ N, 175° 15′ W and 14° 17′ N, 175° 28′ N respectively, perhaps due to the same feature, but not correlated with the bathymetry.

A weak negative signature may be traced across several tracks. The locations and magnitudes are summarized in Table 1. As signature magnitudes we have taken the difference between the central low and the first side lobe. Some tracks have been passed through the wider 400-km filter frequency window (see Figure 1) yielding significantly larger signature magnitudes. Clearly, the 200-km filter has not captured the full signature and we have a rather large scale feature. However, the narrower filter leads to a better separation between features (resolution). This signature may be associated with a slow mesozoic spreading center [8] and signify a trough under the sediment.

TABLE 1. SUMMARY OF SIGNATURES PERTAINING TO THE LONG FEATURE IN FIGURE 6.

Rev. No.	Location	Approximate Low Minus High (cm)	
		N=2, λ=200 km	N=1, λ=400 km
533	11° 41′ N, 179° 26′ W	-40	-70
777	11° 28′ N, 179° 2′ W	-35	-65
619	10° 20′ N, 177° 6′ W	-50	
131	10° 9′ N, 176° 48′ W	-30	
662	9° 33′ N, 175° 58′ W	-15	-50
1293	9° 22′ N, 175° 36′ W	-20	

There is also a weak negative signature on the multiple tracks at about 10° 32′ N, 175° 8′ W of minimum value ~ -20 cm.

We have illustrated an important point:

Correlation across parallel or repeat tracks may reveal weak signatures not otherwise readily apparent above the noise level.

In Figures 4 and 5 we show a bathymetry chart just to the South of that in Figure 2 [7] and data tracks passed through the $N = 3, \lambda = 200$ km filter (see Figure 1) respectively. On track 791 at 4° 21′ N, 172° 52′ W a "Seamount Signature" of maximal value 45 cm is noticeable. It does not correlate with the bathymetry. The large excursions at the data gaps on tracks 102 and 260 are due to filter "End Effects." On track 791 a "Data Error Spike" of -120 cm is noticeable at 6° 32′ N, 171° 59′ W, indicating the utility of high pass filtering for purposes of data editing. This is essential if vertical deflections are to be estimated by automated processing.

In Figures 6 and 7 we have bathymetry [7] and filtered data tracks ($N = 3, \lambda = 200$ km) near the Clipperton Fracture Zone just East of the Christmas Island Ridge. Along the multiple track (thick line) there is a "Seamount Signature" which does not correlate with the bathymetry. Perhaps the ridge to the South-West has been misplaced.

We also notice a negative signature associated with the Clipperton Fracture Zone and extending over all the tracks. It may indicate a trough covered by sediment.

Finally in Figure 8 we show some tracks through the Tasmanian Sea. Two "Seamount Signatures" are apparent. On track 777 the maximal value of the signature is 56 cm at 36° 19′ S, 159° 56′ E. On track 533 the maximal value is 49 cm at 49° 8′ S, 157° 5′ E.

CONCLUSION

We have demonstrated the utility of high pass filtering of satellite altimeter data and presented some results in chart form suitable for overlay on other charts. Full interpretation must await correlation with other data classes, where available. Satellite altimetry constitutes the most extensive data class available over the oceans and furnishes important constraints on crustal models and bathymetry.

REFERENCES

1. Cohen, Charles J. and Bernd Zondek, *Accuracy of Deflection of the Vertical Derived from Satellite Altimetry*, NWL Tech Rpt. TR-2626, October 1971.
2. West, Gladys B., *Smoothing of GEOS 3 Satellite Radar Altimeter Data,* JGR, Vol. 84, No. B8, July 30, 1979, pp 4055–4060.
3. Tapley, B.D., B.E. Schutz and P.A.M. Abusali, *A Sequential Method for Filtering Satellite Altimeter Measurements,* JGR, Vol. 84, No. B8, July 30, 1979, pp 4051–4070.
4. Zondek, B., *Improved Orbit Estimation by Satellite-Mounted Gravity Gradiometers,* Journal of Guidance and Control, Vol. 2, Number 2, May-June 1979.
5. *Digital Processing of Signals,* Bernard Gold and Charles M. Rader, McGraw-Hill, 1969. (Note that the 1st of Eqs 3.40 has a spurious factor of 2).
6. *Digital Filters,* R.W. Hamming, Prentice-Hall, 1977.
7. *Bathymetric Atlas of the North Pacific Ocean,* Scripps Institution of Oceanography, 1978. N.O. Pub. No. 1301-2-3.
8. David Handschumacher, Private Communication.

FIGURE CAPTIONS

Figure 1. Frequency response of some high pass digital Butterworth filters.

T .... Sampling increment

λ .... Wave length

ω .... Circular frequency = $2\pi/\lambda$

Figures 2,4,6. Bathymetry charts taken from [7] in Mid-Pacific Seamount Province, Mid-Pacific and near the Western Clipperton Fracture Zone respectively. These charts are to be overlaid by Figures 3, 5, and 7, respectively.

Figures 3,5,7,8. Bands of subtracks projected on a Mercator grid.

Figure 3 for overlay on Figure 2

Figure 5 for overlay on Figure 4

Figure 7 for overlay on Figure 6

The filtered altimeter data have been plotted perpendicular to the subtracks, so that 1 meter corresponds to the distance between adjacent longitude grid lines in the Mercator grid, i.e., 1 meter $\sim 1°$ longitude. In Figures 3, 5, and 8 positive values lie to the left, in Figure 7 to the right.

FREQUENCY RESPONSE FUNCTIONS

T=3.320 km

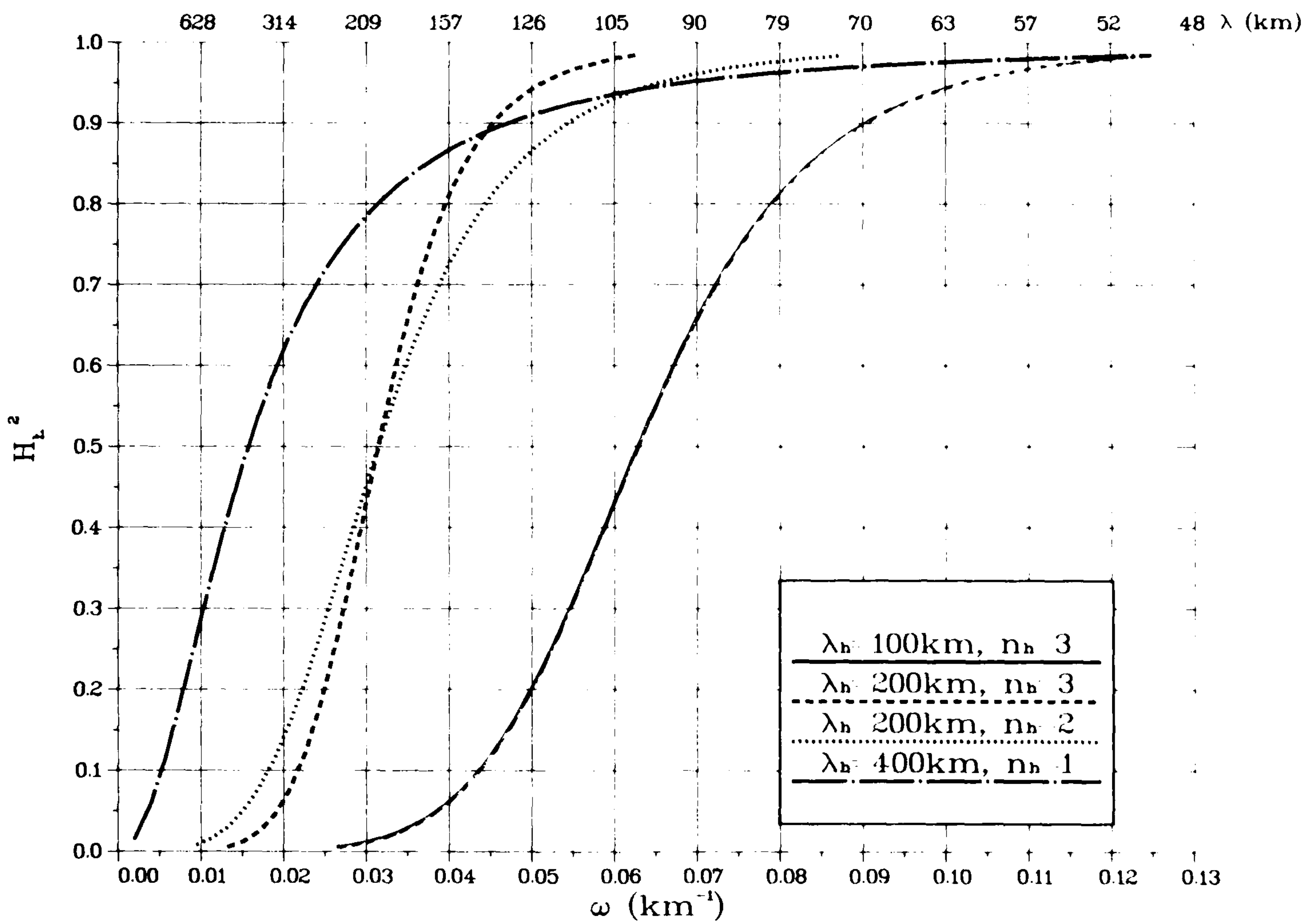

Figure 1.

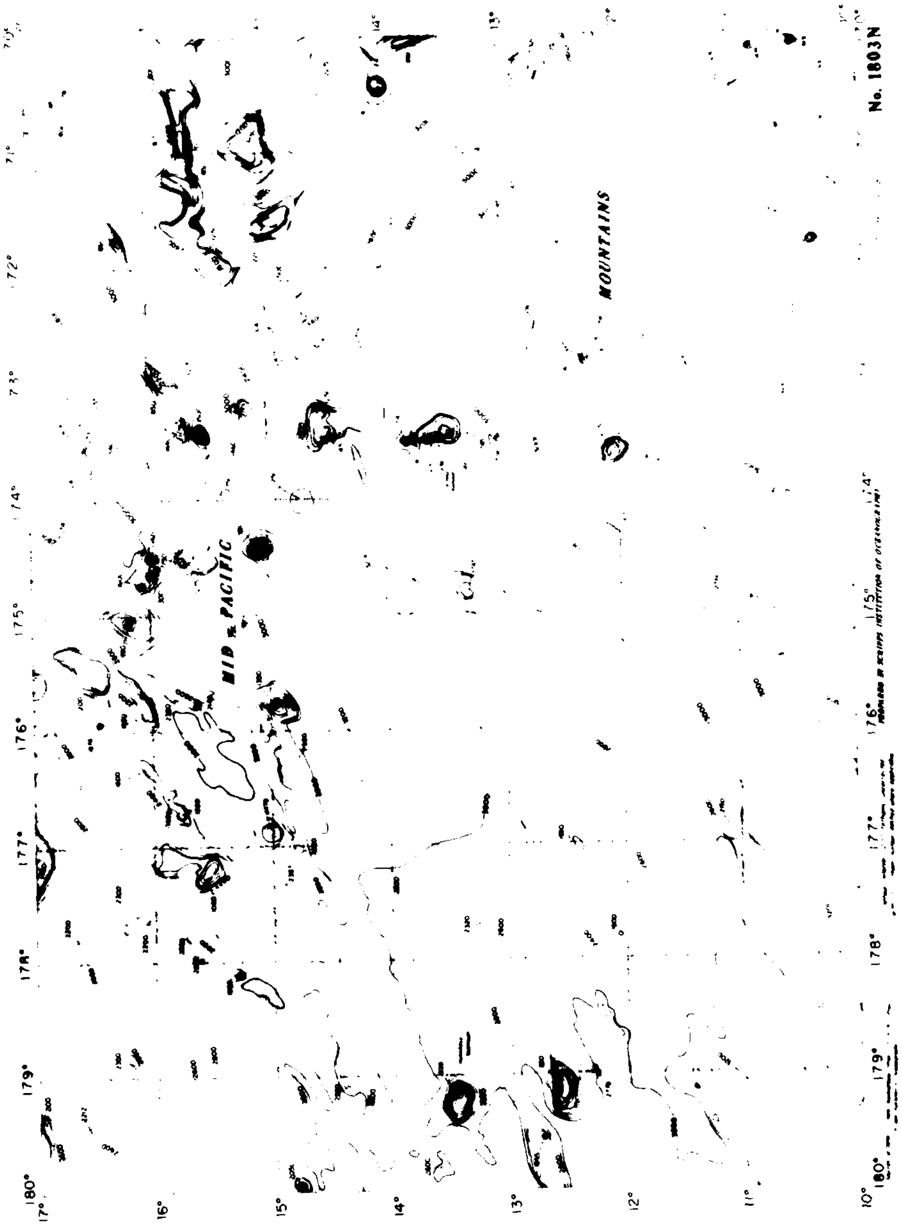

Figure 2.

PRECEDING PAGE BLANK-NOT FILMED

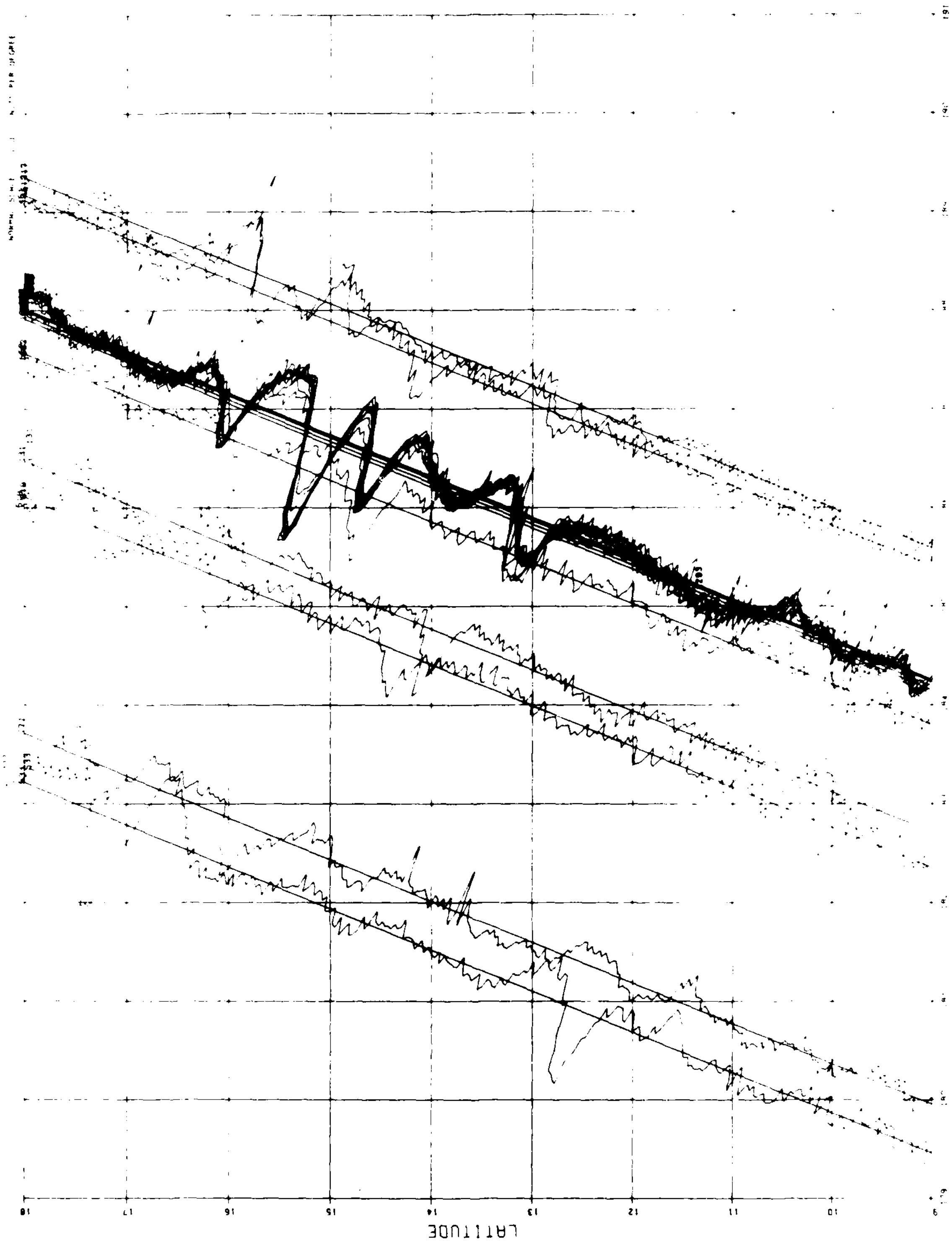

Figure 3.

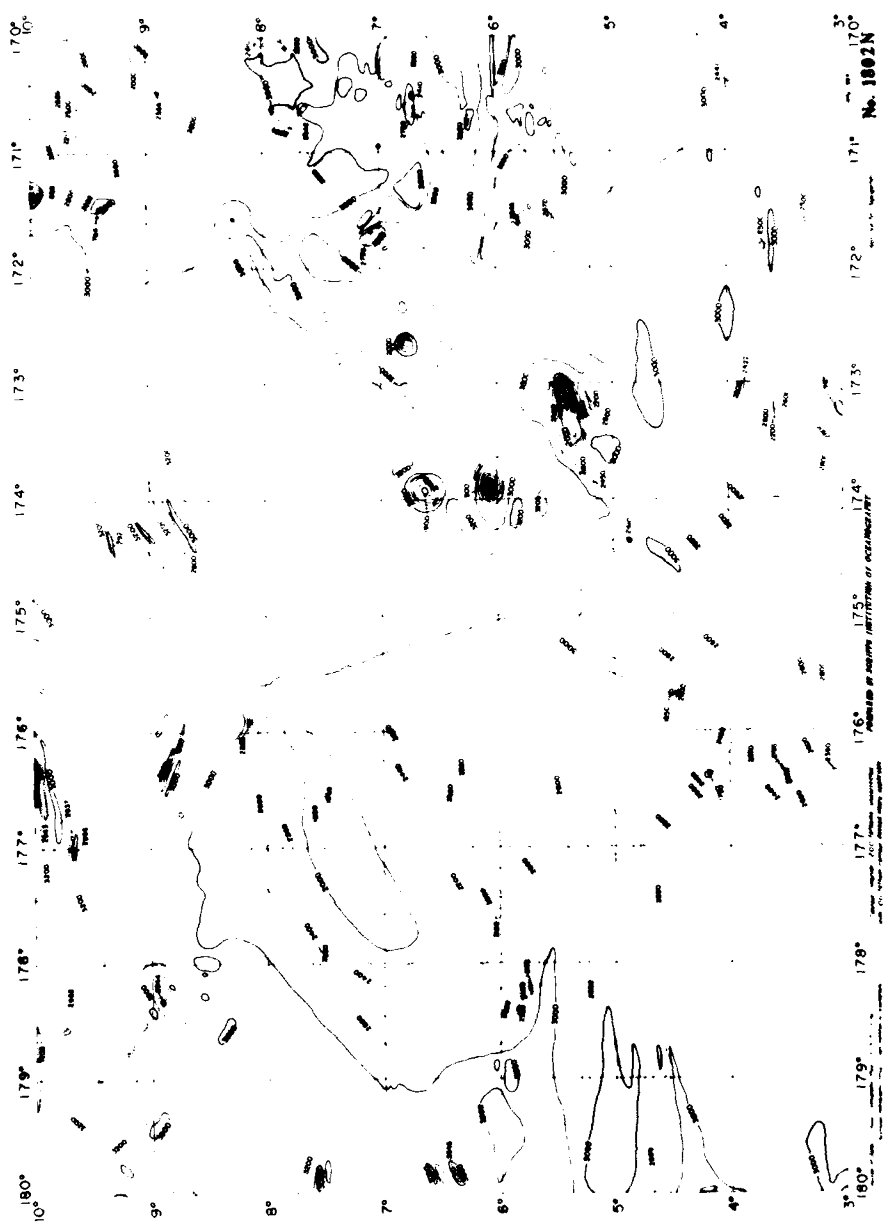

Figure 4.

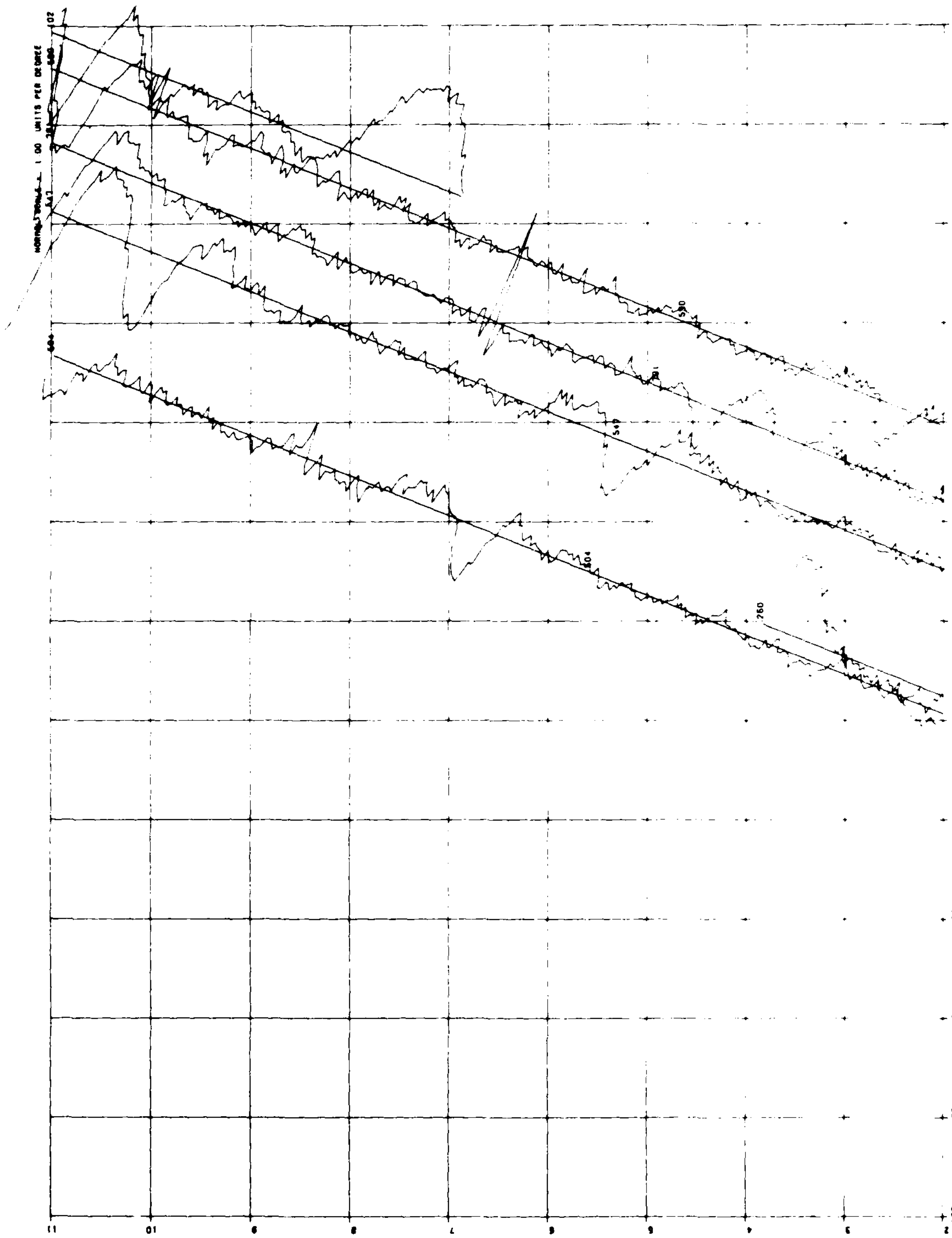

Figure 5.

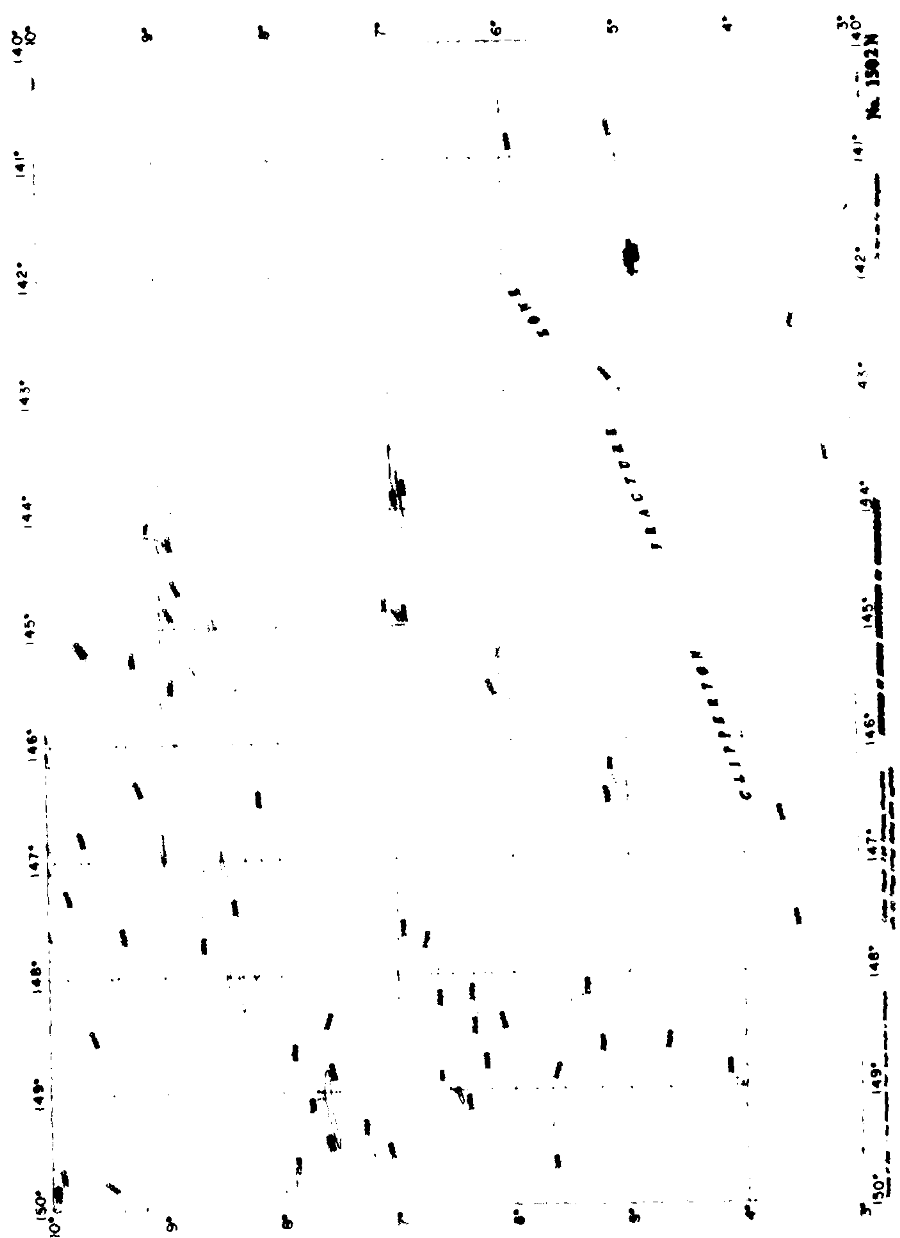

Figure 6.

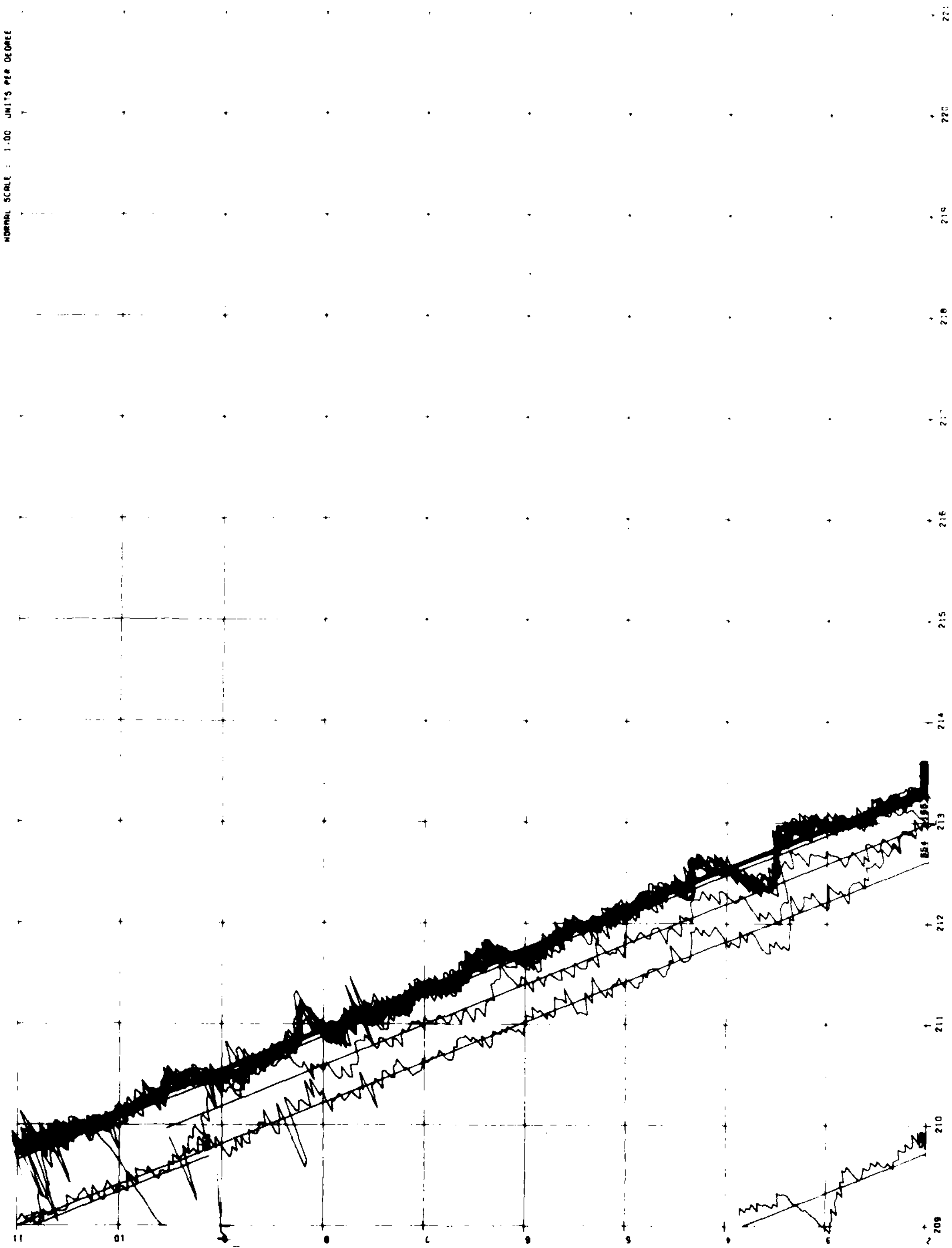

Figure 7.

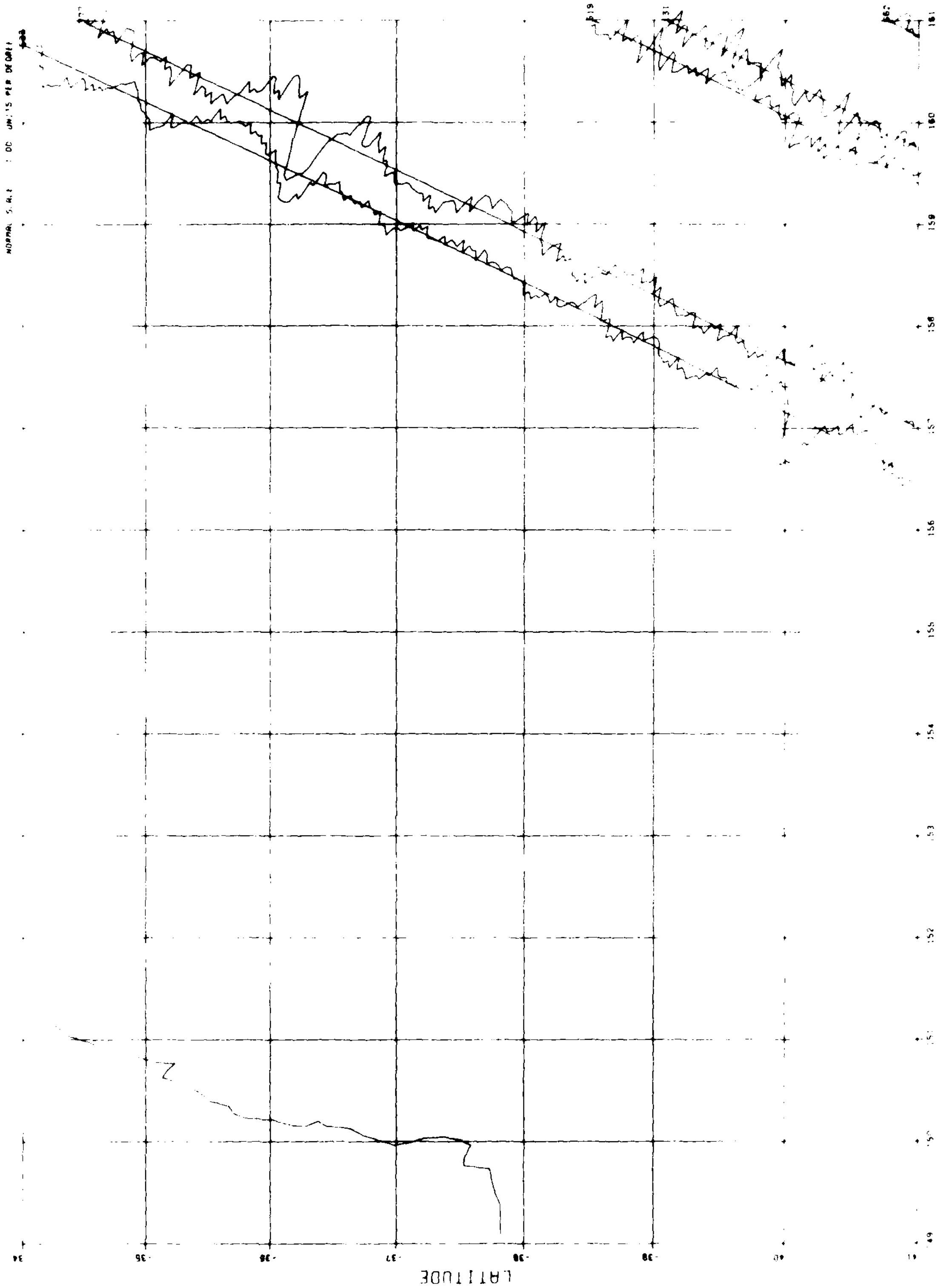

Figure 8.

PRECEDING PAGE BLANK-NOT FILMED

DISTRIBUTION

Oceanographer of the Navy
Hoffman Building 11
200 Stovall Street
Alexandria, Va. 22332

Director, Defense Mapping Agency HQ
Building 56, U.S. Naval Observatory
Washington, D.C. 20305

Director
Defense Mapping Agency
Hydrographic and Topographic Center
6500 Brookes Lane
Washington, D.C. 20315

Director
Defense Mapping Agency
Aerospace Center
St. Louis, Mo. 63118

Defense Documentation Center
Cameron Station
Alexandria, Va. 22314 (12)

Library of Congress
Washington, D.C. 20540
ATTN: Gift and Exchange Division (4)

Local.
E411
E431 (10)
K10
K104 (Zondek) (40)

END

DATE
FILMED

4 – 83

DTIC